Frequency Dependence of the Surface Resistance of Superconducting Tin in the Millimeter Wavelength Region*

R. KAPLAN,† A. H. NETHERCOT, JR.,‡ AND H. A. BOORSE§
Columbia Radiation Laboratory, Columbia University, New York, New York
(Received December 12, 1958; revised manuscript received June 26, 1959)

The ratio of the superconducting to normal surface resistance of polycrystalline tin has been measured at seven frequencies between 17 kMc/sec and 77 kMc/sec and at temperatures from 1.5°K to 3.0°K. These data plus those of other investigators have been compared with the predictions of two theories: the first a calculation made by Serber (unpublished) based on the London two-fluid model of superconductivity and the Reuter-Sondheimer theory of the anomalous skin effect, and the second a calculation based on the Bardeen-Cooper-Schrieffer theory as developed by Bardeen and Mattis.

Agreement between experimental and theoretical results is only fair in the case of the two-fluid theory. The best values of the relevant parameters, Fermi velocity v and mean free path l, were found to be, respectively, $(1.25\pm0.3)\times10^7$ cm/sec and $10^{-3}\rightarrow10^{-1}$ cm. A value of v of approximately 10^8 cm/sec would be expected for tin. The surface resistance ratio from the Bardeen-Cooper-Schrieffer theory has been calculated only for the extreme anomalous limit and the calculation therefore should not apply too accurately for tin. However, a curve of the right general shape is obtained and further calculations more appropriate to tin should improve the agreement between theory and experiment.

I. INTRODUCTION

ONE of the essential features of superconductivity is the vanishing of the dc resistance at the transition temperature. If, however, the surface resistance of a superconductor is investigated at very high frequencies (in the infrared region), experiment[1–4] shows that the resistance remains constant as the temperature is lowered below the transition. Therefore, it would be expected that somewhere in the range of frequencies between zero and the infrared there must be a gradual change between these two limiting conditions. This expectation was first verified by London[5] in 1940, using a frequency of 1.46 kMc/sec. Subsequently, many measurements[6–15] of the superconducting surface resistance have been made in the conventional microwave region, where the surface resistance is large enough to be readily measurable.

In such investigations, it has become customary to make use of the ratio, $r\equiv R/R_N$, where R is the resistance at any temperature in the superconducting state and R_N is the resistance in the normal state just above the transition. These microwave researches show that at any given temperature in the superconducting range, r increases with increasing frequency. A precise knowledge of the frequency dependence of r is useful in testing the validity of theories of superconductivity and as a measure of the parameters, such as mean free path l of electrons and Fermi velocity v, which may appear in such theories. This experiment provides data to find the frequency dependence of r and to determine the parameters v and l.

It is difficult to find the correct frequency dependence of r by the use of data from experiments on different specimens because of the large scatter of the results, even for measurements made at the same frequency. This might be expected since absorption of microwave energy takes place in a very small skin depth and hence is sensitive to the microscopic smoothness of the surface and the degree of strain as well as to the purity of the specimen. The value of R_N is also weakly sensitive to the size of the magnetic fields used to destroy the superconducting state; the results of experiments using different magnetic fields may differ by as much as 10%.[16] Further, if a single crystal of anisotropic material is used, then microwave absorption can vary by as much as a factor of two with orientation of the crystal axes.[13,17]

Because it was evident that microwave absorption measurements were sensitive to the purity and surface finish of the specimen investigated, it seemed most

* Work supported jointly by the U. S. Army Signal Corps, the Office of Naval Research, the Air Force Office of Scientific Research, the National Science Foundation, and the Linde Air Products Company.
† Present address: Department of Physics, University of California, Berkeley 4, California.
‡ Now at the IBM Watson Scientific Laboratory at Columbia University. A part of the work was done while at this location.
§ Pupin Physics Laboratories, Columbia University, New York 27, New York.

[1] Daunt, Keely, and Mendelssohn, Phil. Mag. **23**, 264 (1937).
[2] R. Hilsch, Physik. Z. **40**, 592 (1939).
[3] E. Hirschlaff, Proc. Cambridge Phil. Soc. **33**, 140 (1937).
[4] K. G. Ramanathan, Proc. Phys. Soc. (London) **A65**, 132 (1952).
[5] H. London, Proc. Roy. Soc. (London) **A176**, 522 (1940).
[6] A. B. Pippard, Nature **162**, 68 (1948).
[7] A. B. Pippard, Physica **15**, 40 (1949).
[8] W. Fairbank, Phys. Rev. **76**, 1106 (1949).
[9] I. Simon, Phys. Rev. **77**, 384 (1950).
[10] C. J. Grebenkemper and J. P. Hagen, Phys. Rev. **86**, 673 (1952).
[11] C. J. Grebenkemper, Phys. Rev. **96**, 1197 (1954).
[12] A. A. Galkin and P. A. Bezuglii, Doklady Akad. Nauk. SSSR **97**, 217 (1954).
[13] E. Fawcett, Proc. Roy. Soc. (London) **A232**, 519 (1955); and private communication.
[14] Maxwell, Marcus, and Slater, Phys. Rev. **76**, 1332 (1949).
[15] M. D. Sturge, Proc. Roy. Soc. (London) **A246**, 570 (1958); and private communication.
[16] E. Fawcett, Phys. Rev. **103**, 1582 (1956).
[17] A. B. Pippard, Proc. Roy. Soc. (London) **A203**, 98 (1950).

desirable to make measurements on a single specimen, undisturbed throughout the range of frequencies investigated. Accordingly, a calorimetric method was adopted to determine the absorption. This method has the advantage of providing a direct measurement of the absorbed microwave energy and of requiring no change in the absorbing surface over a wide frequency range. The details are given below in the section describing the apparatus.

II. THEORY

It has been shown[18] that on the basis of any two-fluid model of superconductivity,[19] R must vary as ν^2. In the normal state at sufficiently high frequencies and low temperatures, the mean free path of electrons can be greater than the skin depth. In this case, Ohm's law, which assumes a point relationship between the electric field and the current, is not valid since the field acting on an electron varies significantly over a mean free path. Under these conditions, the electric field and the current must have a nonlocal relationship. This "anomalous skin effect," first calaculated semiquantitatively by Pippard[20] and then rigorously by Reuter and Sondheimer,[21] predicts that R_N will vary as $\nu^{\frac{2}{3}}$ and be independent of temperature. This has been verified experimentally by Chambers,[22] who found that at 3.6 kMc/sec tin was in the anomalous region at temperatures below 8°K. At higher frequencies, the anomalous skin effect sets in at higher temperatures.

Serber (unpublished), using the London two-fluid model of superconductivity and the Reuter-Sondheimer equation for the normal state under anomalous conditions, has calculated the surface impedance, Z, of a superconductor as

$$Z=\frac{8\pi i\nu}{c^2}\int_{-\infty}^{\infty}dk\left[k^2+\frac{\omega_S{}^2}{c^2}-\frac{(2\pi\nu)^2}{c^2}+\frac{3\omega_N{}^2}{4c^2}\frac{2\pi i\nu}{(1+2\pi i\nu\tau)}K(s)\right]^{-1}, \quad (1)$$

where $k=2\pi/\lambda$, $\omega_S{}^2=4\pi n_S e^2/m$, $\omega_N{}^2=4\pi n_N e^2/m$, n_S = density of superconducting electrons, n_N = density of normal electrons, m = effective electron mass, e = electron charge, $\tau=l/v$, l = electron mean free path, v = Fermi velocity, and

$$K(s)=\{2s-(1-s^2)\ln[(1+s)/1-s)]\}s^{-3},$$

with $s=ikl/(1+2\pi i\nu\tau)$. For tin, under the conditions of this experiment, ($t=T/T_c<0.85$ and $\nu<78$ kMc/sec), the value of Z is approximately given by

$$Z=\frac{8\pi^2 i\nu}{c\omega_S}+\frac{24\pi^3\omega_N{}^2\nu^2}{v\omega_S{}^4}f(b), \quad (2)$$

where

$$f(b)=(1-2/b^2)\ln(1+b)-1+2/b,$$

and

$$b=\omega_S l/\{c(1+2\pi i\nu\tau)\}.$$

In the limiting case, $|b|\gg 1$, we obtain $f(b)=\ln b-1$. However, this condition, $|b|\gg 1$, is unnecessarily restrictive since only Re $[f(b)]$ is of interest. If $f(b)$ is expressed in real and imaginary parts, it can be seen that Re $[\ln b-1]$ is a good approximation to Re $[f(b)]$ within a few percent even when $|b|=5$, which is the case at 77 kMc/sec.

Then from Eq. (2),

$$Z=\frac{8\pi^2 i\nu}{c\omega_S}+\frac{24\pi^3\omega_N{}^2\nu^2}{v\omega_S{}^4}\left[\ln\frac{\omega_S l}{c(1+2\pi i\nu\tau)}-1\right], \quad (3)$$

and

$$R=\mathrm{Re}(Z)=-\frac{24\pi^3\omega_N{}^2\nu^2}{v\omega_S{}^4}\left\{1+\frac{1}{2}\ln\left[\left(\frac{\lambda}{l}\right)^2+\left(\frac{2\pi\nu\lambda}{v}\right)^2\right]\right\}, \quad (4)$$

where λ = superconducting penetration depth $=c/\omega_S$.

In this theory, which can be considered a three-parameter two-fluid model, the properties of the superconducting electrons are determined by the parameter λ and the normal properties by the Fermi velocity v and the mean free path l. In the London theory λ_0 and v are considered to be related by $\lambda_0{}^2=3h^3c^2/32\pi m^2v^2$. However, in the following work this relationship will not be used since it is known that it does not lead to the correct penetration depth. Therefore the experimental values of the penetration depth will be used. In this connection, there is an uncertainty as to whether or not the "normal" electrons in a superconductor can be expected to behave in a manner identical to the electrons in a normal metal. Perhaps the low value of the Fermi velocity which is obtained is related to this uncertainty.

In the above expressions it is assumed that the relaxation times and mean free paths of the normal electrons are unaffected by the presence of the superconducting electrons and are therefore practically temperature independent. The important parameter determining the high-frequency behavior is the ratio λ/v or $\lambda\tau/l$. This parameter becomes effective when $\omega\tau=\omega l/v\approx 1$, (somewhere between 100 → 1000 Mc/sec), but the magnitude of the effect in the microwave region

[18] A. B. Pippard, Proc. Roy. Soc. (London) **A203**, 195 (1950).
[19] F. London, *Superfluids* (John Wiley and Sons, Inc., New York, 1950), Vol. 1.
[20] A. B. Pippard, Proc. Roy. Soc. (London) **A191**, 385 (1947).
[21] G. E. H. Reuter and E. H. Sondheimer, Proc. Roy. Soc. (London) **A195**, 336 (1948).
[22] R. G. Chambers, Proc. Roy. Soc. (London) **A215**, 481 (1952).

depends primarily on the ratio $\omega\lambda/v$ and is roughly independent of l.

As is evident from Eq. (4), the frequency dependence of the superconducting surface resistance is proportional to ν^2 at low frequencies, and then increases less rapidly with frequency at higher frequencies because of the presence of ν in the logarithmic term. The temperature dependence of R is primarily determined by the ratio $\omega^2_N/\omega_S{}^4$. Much smaller effects are produced by the temperature variation of λ, l, and v in the logarithmic term. In this range the temperature variation of l and v are infinitesimally small and the effect produced by the variation of λ is also small. The variation in λ with temperature up to the highest temperature used in the experiment ($t\approx 0.8$) is approximately 30% and this variation is too little to sensibly affect the results. Therefore it will be assumed that only $\omega^2_N/\omega_S{}^4$ varies with temperature and that the surface resistance R can be expressed as a product of temperature-dependent and frequency-dependent functions.

Since the resistance of the normal metal, R_N, is proportional to $\nu^{\frac{2}{3}}$ and independent of temperature, we obtain $r=R/R_N=A(\nu)\varphi(t)$:

$$r=-K'\nu^{\frac{2}{3}}\{1+\tfrac{1}{2}\ln[(\lambda/l)^2+(2\pi\nu\lambda/v)^2]\}\varphi(t). \quad (5)$$

Thus,[23] r should be proportional to $\nu^{\frac{2}{3}}$ at low frequencies ($\omega\ll v/l$), but should deviate from this simple power law when the frequency is sufficiently high ($\omega\approx v/l$).

The value of $K'\varphi(t)$ may be deduced from the Serber theory as $60[t^4/(1-t^4)^2](c^2m/v^2 4\pi ne^2)^{\frac{2}{3}}$, a quantity which depends on the electronic mass and charge and particularly on the total number of conduction electrons per unit volume as well as on the Fermi velocity. It has been found experimentally[17] that the temperature dependence is more closely $\varphi(t)=t^4(1-t^2)/(1-t^4)^2$ than $t^4/(1-t^4)^2$ and the former function is generally used rather than the latter in the computation of $A(\nu)$ from the experimental values of r.

It is also possible to predict the behavior of the superconducting surface resistance ratio from the BCS (Bardeen-Cooper-Schrieffer) theory.[24] Integral expressions for σ_1/σ_N and σ_2/σ_N (where $\sigma_1-i\sigma_2$ is the complex conductivity in the superconducting state and σ_N that in the normal state) are given in the paper of Mattis and Bardeen[25] [see Eqs. (3,9) and (3,10)]. Numerical integration of these equations has been carried out by Miller[26] for the extreme anomalous limit (coherence distance much larger than the penetration depth). This is not a good approximation for tin. The calculations are now being extended so they can be used for tin, but in the interim it is of some interest to compare the presently available theoretical results to the experimental even if the theoretical results are not expected to apply exactly. The impedance is calculated from the expression $Z_{\infty S}/Z_{\infty N}=[(\sigma_1-i\sigma_2/\sigma_N)]^{-\frac{1}{3}}$.

[23] An expression for r having the same form as Eq. (5) at $t=0$ has been obtained by Maxwell, Marcus, and Slater.[14] However, at $t>0$, their expression for r is in a form which is difficult to apply to the experimental data.

[24] Bardeen, Cooper, and Schrieffer, Phys. Rev. **108**, 1175 (1957).

[25] D. C. Mattis and J. Bardeen, Phys. Rev. **111**, 412 (1958).

[26] P. B. Miller (private communication).

III. APPARATUS AND EXPERIMENTAL METHOD

The arrangement of the apparatus in the cryostat is shown schematically in Fig. 1. The Pyrex Dewar, D, containing liquid nitrogen, surrounds the brass container, C, which, in operation is pumped to a high vacuum (pumping tube not shown). The inner containers, B and A, both of brass, serve, respectively, as the liquid helium reservoir (capacity 1.6 liters) and the experimental chamber.

The temperature of the helium bath is regulated in the usual way by pumping (pump tube not shown), and the temperature is determined by vapor pressure measurements. The vapor pressure tube, I, extends to the bottom of the helium bath and is connected outside the cryostat to two manometers at room temperature, one containing mercury and the other butyl sebacate. The latter manometer was used for pressure measurements at less than 7 cm of mercury. In both cases, temperature corrections to the density of the liquid were made. The 1955 Leiden temperature scale was used and liquid helium pressure head corrections were made

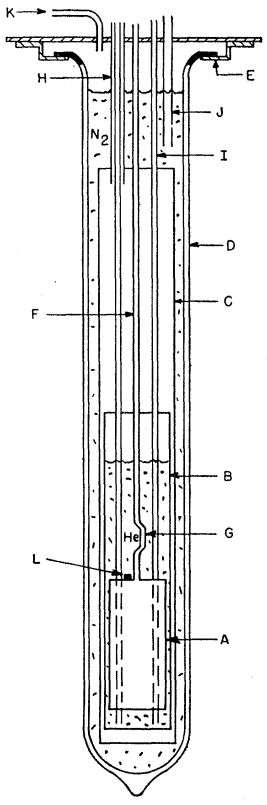

FIG. 1. Cryostat: Schematic representation of significant components showing: (A) experimental chamber, (B) helium bath chamber, (C) helium isolation vacuum chamber, (D) Pyrex Dewar vessel, (E) support flange, (F) waveguide, (G) bend in waveguide, (H) helium transfer tube, (I) helium vapor pressure tube, (J) liquid nitrogen filling tube, (K) liquid nitrogen exhaust tube, (L) carbon resistance thermometer. Pump tubes are not shown.

above the lambda point. In order to maintain a constant bath temperature, a manostat, which operated a solenoid valve in the helium bath pump line, was coupled into the mercury manometer. At pressures of less than 7 cm of mercury, the operation of the manostat was unsatisfactory and constant temperature was maintained by manual adjustment of the valves in the helium bath pump line.

The section of K-band waveguide, F, inside the cryostat was made of an 80% copper–20% nickel alloy with 0.040-inch wall thickness. This material has low thermal conductivity at liquid helium temperatures.

A drawn layer of silver, 0.001 inch thick, lined the inside of the waveguide in order to reduce the dissipation of microwave power in the walls. Just above the liquid helium bath, the waveguide walls were turned down to a thickness of 0.025 inch on the broad sides and 0.015 inch on the narrow sides over a length of one inch, and the silver coating was removed in order to reduce still further the heat leak from the liquid nitrogen bath to the liquid helium bath. Just above the experimental chamber, the waveguide was bent to one side and then back again, as shown at G, so that there was no line-of-sight path for thermal radiation from room temperature and liquid nitrogen regions to the specimen. Outside the cryostat, at room temperature, the copper-nickel waveguide was connected to standard waveguide with a flange joint. A mica window with lead gaskets provided a vacuum seal at this point. Inside the experimental chamber the waveguide was terminated by a one inch square brass horn (see Fig. 2). Another mica window was placed over the end of this horn to prevent any "hot" molecules that might be desorbed from the walls of the waveguide from reaching the specimen; however, there was no vacuum seal at this window.

The specimen, shown in Fig. 2, was a tin cylinder 4.25 cm in diameter and 2.50 cm high. The purity of the specimen was given by the supplier, Vulcan Detinning Company, Sewaren, New Jersey, as 99.9995+ %. After being cast in glass, the specimen was machined to

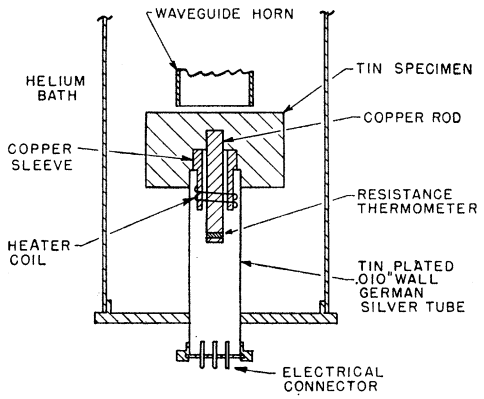

FIG. 2. Experimental chamber containing tin specimen with thermometer and heater.

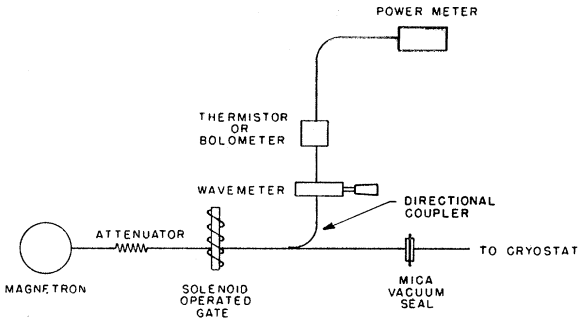

FIG. 3. Schematic diagram of microwave system.

size, annealed, and the surface was lightly etched. The crystallites in the specimen could then be seen, being about 2–4 mm in size. The surface was then given a very light finishing cut in a lathe.

The thermometer, a nominal $\frac{1}{10}$ watt 39 ohm Allen-Bradley carbon resistor, was cemented into a hole in an OFHC copper rod, which was then cemented into a hole in the specimen. A heater coil of German silver wire of diameter 0.0025 inch was wound noninductively and cemented to an OFHC copper sleeve, which was then cemented into a coaxial hole in the specimen. The heater resistance was 152 ohms at room temperature and 135 ohms at liquid helium temperatures.

The specimen was supported by a German silver tube of 0.010-inch wall thickness and 3.1 cm long. A tin plating approximately 2.5×10^{-5} cm thick (about four times the superconducting penetration depth at the highest temperatures used in this experiment) covered the outer surface of the support tube so that any stray radiation in this region would be incident upon a surface of the same material as the specimen. At the upper end of the tube, a pure tin solder joint was made by heating the specimen adjacent to the tube. The joint at the lower end of the tube was made with ordinary soft solder. Wires from the thermometer and heater passed down the inside of the support tube to a vacuum tight electrical connector. From this connector, they passed through the surrounding helium bath, up the helium bath pump tube to another vacuum tight electrical connector, and then out of the cryostat to the measuring circuits via shielded cables. The spacing between the waveguide horn and the specimen was approximately $\frac{1}{32}$ inch. The upper surface of the specimen was aligned perpendicular to the axis of the horn by eye. Two glass capsules (not shown) packed with steel wool were connected to the lid of the experimental chamber. The steel wool acted as a microwave absorber, damping any radiation that leaked out between the horn and the specimen. The capsules were open to the helium bath and were always filled with liquid helium, which carried away any heat developed in the steel wool. An electromagnet with a 6.75-inch pole gap and 2.75-inch pole face diameter was used to

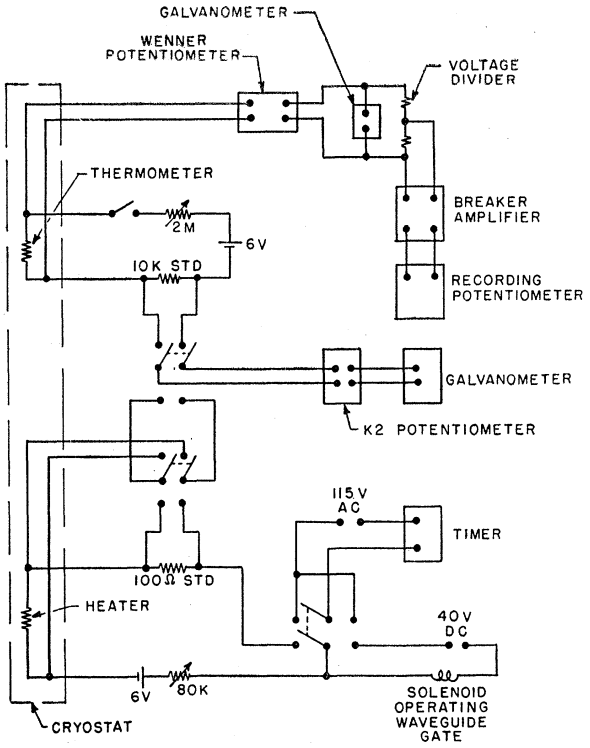

FIG. 4. Schematic diagram of measuring circuits.

destroy superconductivity. It produced a horizontal field of 900 gauss in the region of the specimen.

A schematic diagram of the microwave system is shown in Fig. 3. The gate consisted of a solenoid-operated attenuator which could be inserted into a slot cut in the broad side of the waveguide. This attenuator absorbed approximately 99% of the incident power. In order to avoid the possibility of a magnetron frequency shift that might occur if the power output were varied by changing the operating voltages, the magnetrons were operated under fixed stable high power conditions. The power reaching the specimen was varied by inserting different attenuators in the waveguide. These attenuators consisted of waveguide sections six inches long painted on the inside with an iron powder-lacquer mixture. The thickness of the coating determined the attenuation of the section. The directional couplers used had a coupling constant of 20 db and a directivity of 40 db. Thermistors were used to measure microwave power at K-band frequencies; bolometers were used at the higher frequencies. A self-balancing direct-reading power meter, FXR Machine Works type B830A, was connected to the detector being used.

The thermometer and dc heater measuring circuits are shown in Fig. 4. A measuring current of 10 microamperes was used in the thermometer circuit. Since the series resistance in the circuit was always much larger than the thermometer resistance, the 10-microampere current did not change significantly with small temperature changes. Before a measurement was begun, the Leeds and Northrup Wenner potentiometer was set slightly off balance. A Liston-Becker dc breaker amplifier, model 14, was used to amplify the off-balance voltage from the Wenner potentiometer; this provided an accurate measurement of the change of thermometer resistance. A voltage divider between the amplifier and the Wenner potentiometer was required in order to avoid overloading the amplifier. In order to eliminate pickup from the magnetron pulse generator, it was necessary to shield all the measuring circuits and to insert filters in the thermometer cables.

Since the specimen was always slightly warmer than the helium bath, the recording potentiometer drifted slowly in the cooling direction. When the galvanometer indicated that the Wenner potentiometer was in balance, the thermometer resistance was recorded and the microwave or dc power was turned on for about ten seconds. As the specimen warmed, the recording potentiometer moved in the warming direction. When the power was turned off, the recording potentiometer indicated cooling again. A typical heating trace is shown in Fig. 5. The temperature rise was found by extrapolation of the fore- and after-periods to the center of the heating interval and measurement of the deflection at that point. The recording potentiometer was calibrated by measurement of the deflections caused by known off-balance voltages from the Wenner potentiometer.

The switch which was used to operate the waveguide gate and dc heater also operated a precision electric timer which could be read to 0.01 second. A Leeds and Northrup $K2$ potentiometer was used to measure the thermometer current, the heater current, and the heater voltage.

The magnetrons used for generating microwave power were all fabricated in the Columbia Radiation Laboratory with the single exception of the 34.71-kMc/sec tube, which was a Microwave Associates, Inc. tube, type 5789. All the tubes were operated at 500, 1000, or 2000 pulses per second and a pulse width of 0.3 microsecond. A Raytheon type WX 4053A power supply and type EX4054B modulator were used to operate

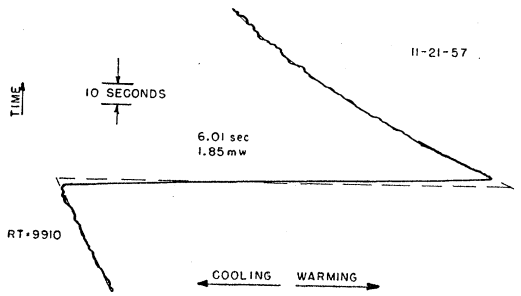

FIG. 5. Typical recording potentiometer trace for microwave heating.

the magnetrons of 34.71 kMc/sec and higher frequencies, and a General Electric power supply type GEI-16067 and Experimental Service Modulator Model 4, type 1372, were used with the lower frequency magnetrons. A small permanent magnet was used to operate these lower frequency magnetrons, and an electromagnet was used with the higher frequency magnetrons.

IV. RESULTS

When the specimen absorbs microwave energy, the absorption coefficient, a, may be defined as

$$a=H\Delta T/p\tau, \tag{6}$$

where H is the heat capacity of the specimen, ΔT is the temperature rise, p is the power incident on the specimen, and τ is the time of heating. The specific heat is known from other experiments[27] and ΔT and τ are measured. From the value of R_N obtained by Grebenkemper and Hagen,[10] values of a_N were calculated at each of the frequencies used in this experiment by the anomalous skin effect relation

$$a_N \propto R_N \propto \nu^{\frac{2}{3}}.$$

The values of a_N thus obtained were all smaller than the corresponding values of a_N obtained from Eq. (6), if it is assumed that the power incident on the specimen is the power measured at the detector. This difference was ascribed to the leakage of radiation into the experimental chamber and its incomplete absorption by the steel wool absorbers. Hence, the expression for a must be modified to

$$a=\beta H\Delta T/P\tau, \tag{7}$$

where P is the power measured at the detector and β is a factor which depends on the frequency. The values of β at the frequencies employed are given in Table I.

At a fixed temperature and frequency, several measurements of P, ΔT, and τ were made in the normal state, then in the superconducting state, and then again in the normal state. During this time, the frequency was monitored. If the frequency shifts were negligible and if the two groups of normal data agreed, it was assumed that β had remained constant. Under these circumstances, r may be evaluated as follows:

$$r=R/R_N=a_S/a_N=(c\Delta T/P\tau)_S/(c\Delta T/P\tau)_N, \tag{8}$$

where c_S and c_N are the superconducting and normal specific heats, respectively. Hence, β does not appear in the expression for r.

TABLE I. Leakage radiation factor, β, as a function of frequency.

ν(kMc/sec)	β	ν(kMc/sec)	β
16.90	13	34.71	22
21.91	2.3	46.96	46
21.91	2.3	70.84	5.0
24.01	1.0	77.38	12
24.01	16		

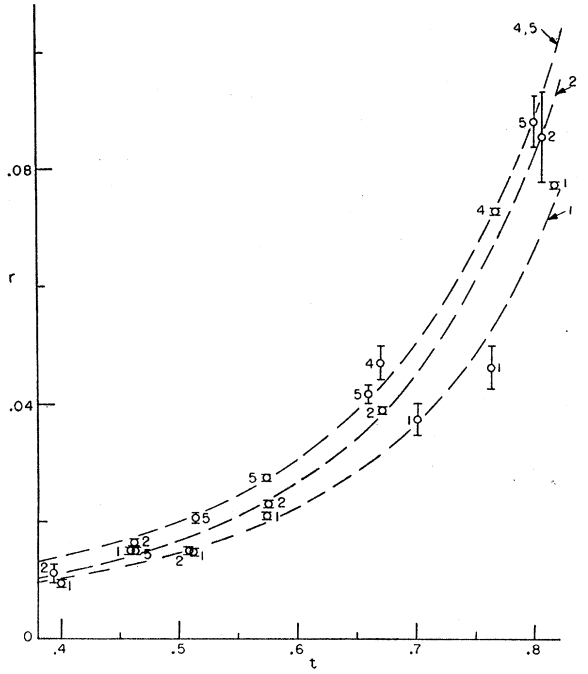

FIG. 6. Measured values of r as function of t: (1) 16.90 kMc/sec, (2) 21.91 kMc/sec, (4) 24.01 kMc/sec, (5) 24.01 kMc/sec.

The validity of this treatment of the factor, β, may be verified by an examination of the data. The value of β was greatest at 46.96 kMc/sec. Nevertheless, the scatter of the data at this frequency was smaller than at any other frequency used in this investigation. Furthermore, although the values of β at 24.01 kMc/sec were 1.0 and 16 for two different runs on two different days, the values of r for these two runs fell on the same curve. Hence, it may safely be concluded that the measurement of r was not measurably affected by the leakage radiation.

The measured values of r are shown in Figs. 6 and 7 as a function of t. (The maximum and minimum values of r shown at each value of t correspond to the values of r obtained using the values of R_N measured before and after the measurement of R.) The broken line curves in these figures correspond to the straight lines obtained in the r *vs* $\varphi(t)$ graphs described below, except that r is here plotted against t.

Pippard[6] found that, if at a given frequency r is plotted against the empirical function

$$\varphi(t)=t^4(1-t^2)/(1-t^4)^2,$$

a straight line is obtained for $t<0.85$. This expression has been found to hold for all frequencies up to 24

[27] W. S. Corak and C. B. Satterthwaite, Phys. Rev. **102**, 662 (1956).

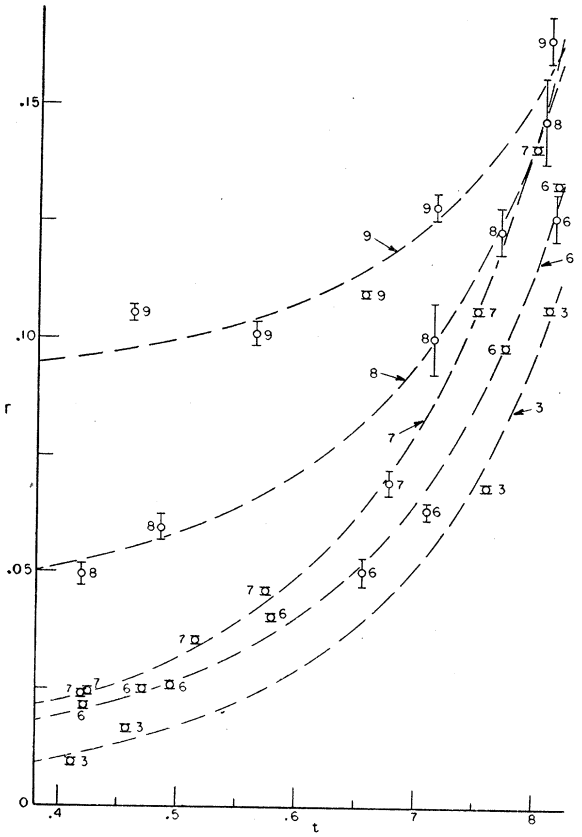

FIG. 7. Measured values of r as a function of t: (3) 21.91 kMc/sec, (6) 34.71 kMc/sec, (7) 46.96 kMc/sec, (8) 70.84 kMc/sec ($\times\frac{1}{2}$), (9) 77.38 kMc/sec ($\times\frac{2}{5}$).

kMc/sec. Fawcett,[13] however, has noted some deviation from this relationship at low temperatures at 36 kMc/sec. In order to analyze the present data, the assumption has been made that a straight line is obtained at the frequencies and temperatures used in this experiment. This was found to be the case within experimental error. Accordingly, from Eq. (5), with $t<0.85$, r may be expressed by the relation

$$r=A(\nu)\varphi(t)+r_0. \tag{9}$$

Here r_0, the residual resistance ratio, is included in order to take account of the anomalous nonvanishing resistance observed at $t=0$. A nonvanishing frequency-dependent r_0 has been observed in all the microwave experiments to date. However, since the origin of this effect is not understood, its inclusion as an additive constant is a hypothesis, albeit a reasonable one made in all the previous experiments.

TABLE II. Frequency-dependent part of r and extrapolated value of r_0.[a]

ν(kMc/sec)	$A(\nu)$	r_0
16.90	0.141±0.006	0.0071±0.0014
21.91	0.179±0.003	0.0071±0.0006
21.91	0.215±0.008	0.0054±0.0022
24.01	0.193±0.001	0.0097±0.009
34.71	0.241±0.004	0.0140±0.0012
46.96	0.301±0.004	0.0158±0.0008
70.84	0.457±0.008	0.0925±0.0023
77.38	0.358±0.036	0.2301±0.0093

[a] Probable errors were computed from the data by the method of least squares.

Graphs of r *vs* $\varphi(t)$ have been plotted for all the frequencies used and straight lines fitted to the points by the method of least squares. $A(\nu)$ is the slope of these lines.

A typical graph is shown in Fig. 8. The two points shown at each value of $\varphi(t)$ correspond to the values of r obtained using the values of R_N measured before and after the measurement of R. The value of the residual resistance ratio, r_0, was obtained by extrapolating these straight lines to absolute zero. The values of $A(\nu)$ thus obtained are given in Table II.

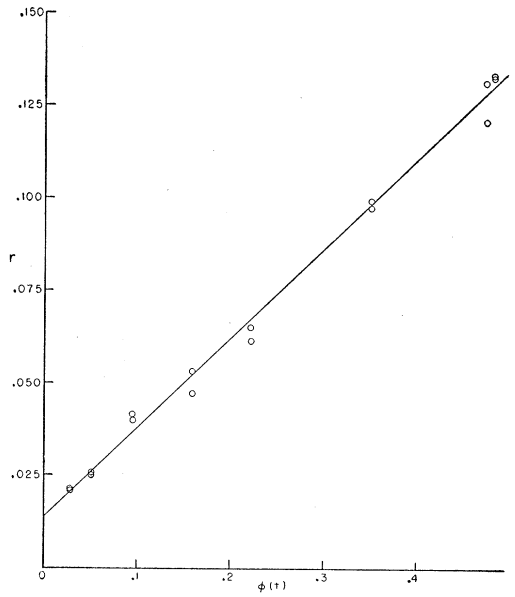

FIG. 8. Measured values of r as a function of $\varphi(t)$ at 34.71 kMc/sec.

Determination of $\varphi(t)$ requires a knowledge of the transition temperature. The heat capacity of tin, like that of all pure superconductors, is characterized by a large discontinuity at the transition temperature. This discontinuity was observed at (3.710±0.008)°K, which was therefore taken to be the value of T_c.

The values of r_0 *vs* ν are also shown in Table II. The value of r_0 is fairly constant at the lower frequencies, but rises sharply at the higher frequencies. Although it is not clear why this variation occurred, such behavior has been observed by other investigators.

In Figs. 9, 10, and 11 the measured values of $A(\nu)$ are plotted against ν. Both the present data and the results obtained in other laboratories are included. In the cases where the previous data were taken on a

single-crystal specimen, a direct comparison to the present data on a polycrystalline sample cannot be made. Therefore, the single-crystal results were averaged over all orientations so that they would correspond to the results for a random polycrystalline aggregate. The data of Fawcett[13] on the anisotropy of $A(\nu)$ were used for this purpose.

It should also be mentioned that the point at 70.84 kMc/sec (which lies high) is suspect since the apparent absorption coefficient changed by a factor outside the experimental error during the run. The reasons for this occurrence were unknown.

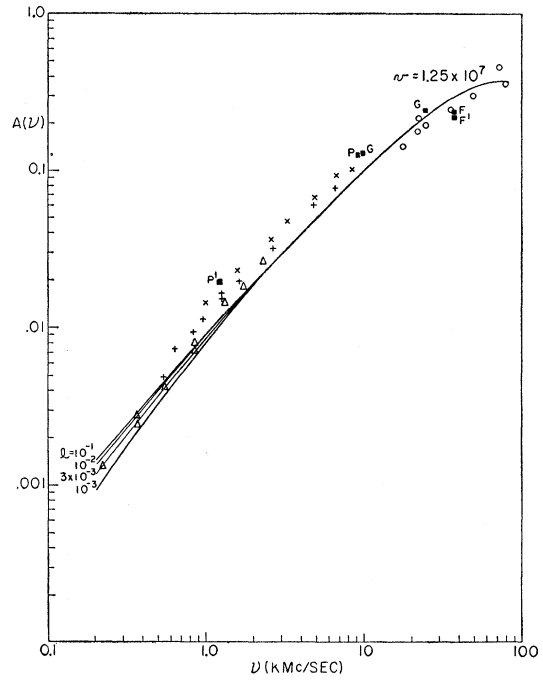

FIG. 9. $A(\nu)$, frequency-dependent part of r, as a function of frequency. o-this experiment; ×, +, △-Sturge[15] (three different averaged single crystals); P-Pippard[17] (averaged single crystal); P'-Pippard[18] (polycrystal); G-Grebenkemper[11] (polycrystal); F-Fawcett[13] (averaged single crystal); F'-Fawcett[13] (polycrystal). The theoretical curves shown are calculated from Eq. (5) with the Fermi velocity $v=1.25\times10^7$ cm/sec and various values of mean free path, l.

V. DISCUSSION

The data of Sturge shows a variation of the surface resistance ratio as the four-thirds power of the frequency at frequencies below 1.5 kMc/sec. At higher frequencies, the points fall below the four-thirds power law line as predicted theoretically. Since it is necessary to use both high-frequency and low-frequency data to determine values of the parameters, v and l, which occur in the two-fluid theory, all the data from 0.2 to 77.4 kMc/sec must be included. Therefore, a single curve is drawn through all the points available. Although data on different samples are included, it is seen in Figs. 9, 10, and 11 that all the best data available does lie

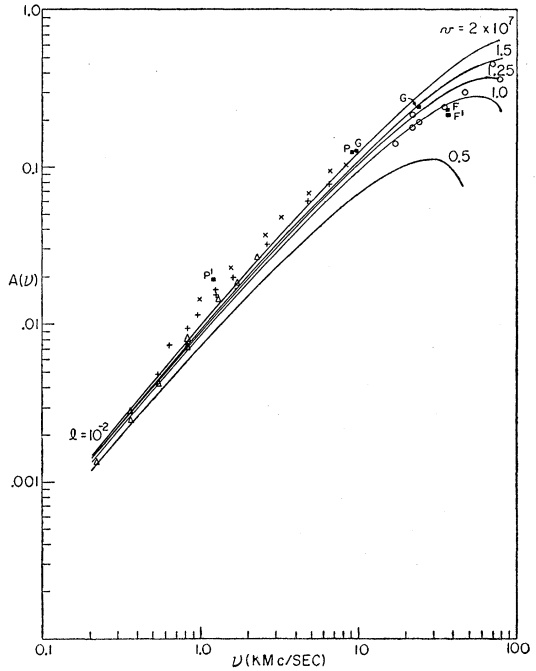

FIG. 10. $A(\nu)$, frequency dependent part of r, as a function of frequency. The points are identical with those shown in Fig. (9). The theoretical curves shown are calculated from Eq. (5) with $l=10^{-2}$ cm and various values of v.

approximately on a single curve. However, the present data seems to fall somewhat lower than that of Sturge.

Theoretical curves were calculated from Eq. (5) for various values of the parameters λ, l, and v. It was found, for any reasonable value of λ (see Table III),[24,28–31] that the best values of l or v were not appreciably affected. The value adopted for λ was 5.0×10^{-6} and

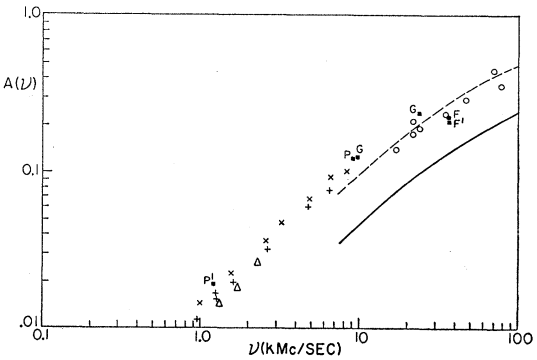

FIG. 11. $A(\nu)$, frequency dependent part of r, as a function of frequency. The points are identical with those shown in Fig. 9. The solid theoretical curve shown is calculated from the BCS theory as given by Mattis and Bardeen.[25] The dashed curve is the same, but multiplied by the factor 2.0.

[28] R. G. Chambers, Proc. Cambridge Phil. Soc. **52**, 363 (1956).
[29] J. M. Lock, Proc. Roy. Soc. (London) **A208**, 391 (1951).
[30] A. B. Pippard, Proc. Roy. Soc. (London) **A191**, 399 (1947).
[31] E. Laurmann and D. Shoenberg, Proc. Roy. Soc. (London) **A198**, 560 (1949).

TABLE III. Values of λ_0 for tin quoted in the literature.

Reference	λ_0 (cm)	Type of specimen
28	4.3×10^{-6}	Average of single crystals
29	5.0×10^{-6}	Thin films
30	5.0×10^{-6}	Polycrystal
31	5.2×10^{-6}	Average of single crystals
24	5.67×10^{-6}	Calculated

it was assumed as described previously that λ was independent of temperature up to the highest temperature used ($t=0.8$); the variation in λ of perhaps 30% over this temperature range is not sufficient to cause appreciable errors. Curves were plotted for various values of v with l equal to 10^{-2} cm and also for various values of l with $v=1.25\times10^7$ cm/sec. If the constant K' in Eq. (5) is considered an adjustable constant, the theoretical curves and experimental points when plotted on a logarithmic scale can be moved vertically with respect to each other. In Figs. 9 and 10 it is seen that it is not possible to fit the theoretical and experimental points exactly merely by adjustment of the constant K' or by changes in l and v. Therefore, the results do not accurately obey the two-fluid model. However, if v is chosen to be 1.25×10^7 cm/sec and l to be between 10^{-3} and 10^{-1} cm, the experimental points are all within approximately 20% of the theoretical curve. Only this value of the parameter $v=(1.25\pm0.3)\times10^7$ cm/sec gives a reasonable fit with the data. Since the Fermi velocity is expected to be about 10^8 cm/sec, it is seen that either the two-fluid picture of a degenerate gas of electrons cannot be taken at its face value or the theory is not correct.

A mean free path of about 10^{-3} cm fits the shape of the low-frequency data better, but, if the multiplying constant K' is adjusted to match the present high-frequency data, $A(\nu)$ is then too small at the lowest frequencies. A value of l between 10^{-1} and 10^{-2} cm fits both the highest and lowest frequency data better, but not the intermediate-frequency data. In cyclotron resonance investigations on tin[32] a relaxation time, τ, of up to 150×10^{-11} sec was observed at 4°. From the relation $l=\tau v$, a value of $l=2\times10^{-2}$ cm is then derived. Other values of l in the literature are 10^{-2} cm as given by Pippard[33] and more recently a value of 6.5×10^{-2} cm has been reported.[34] It should be emphasized that some of the difficulty in determining l may arise from the artificial joining of data on several specimens. This might raise or lower one end of the curve relative to the other. However, the value of v is determined primarily by the shape of the high-frequency data and therefore should be relatively unaffected by such difficulties.

The value of K' in Eq. (5) is given by theory as $60(c^2m/v^2 4\pi ne^2)^{\frac{2}{3}}$ and hence depends on the electronic charge and mass, the Fermi velocity, and the density of conduction electrons. If the charge and mass of free electrons and a Fermi velocity of 1.25×10^7 cm/sec are used, the density, n, which fits the absolute value of $A(\nu)$ corresponds to 0.25 electrons per tin atom. This number seems rather low and casts further doubt on the interpretation of the two-fluid model calculation.

It is also possible to compare the experimental results with the results of the BCS theory[24] as explained earlier. Figure 11 shows both the experimental points and the surface resistance ratio derived from the values of σ_1/σ_N and σ_2/σ_N calculated by Miller[26] from the integral relations of Bardeen and Mattis.[25] It is seen that the right general shape is predicted, but that the absolute value lies below the experimental observations. However, this calculation was made for the extreme anomalous limit (coherence distance much larger than the penetration depth) and this is not a good approximation for tin. A preliminary calculation[26] for tin has shown that r will be increased by a large factor, perhaps even 100% or more, above the extreme anomalous limit value at the frequency $\hbar\omega\approx kT_c$. This modification reduces the discrepancy in absolute value and may also alter the shape somewhat.

The BCS theory does not consider anisotropy at present and the zone structure of tin is very complicated. $A(\nu)$ and R_N both show very considerable anisotropy. $A(\nu)$ for a single crystal of tin can vary from $0.7\rightarrow1.7$ times that for polycrystalline tin. Therefore, it is not clear which experimental value should be compared to the theoretical value. However, it appears the two will overlap when the revised calculation is available. It should be pointed out that this theory involves no undetermined parameters while the two-fluid calculation really involves three (λ/l, λ/v, and n), the derived values of which do not appear very reasonable. Therefore, it can be said that the BCS theory describes the experimental observations as well or better than the two-fluid model calculation.

The highest frequency used in this experiment was 77.38 kMc/sec (corresponding to $1.0kT_c$). At the highest temperature used, 3.0°K, the energy gap predicted by the theory of Bardeen, Cooper, and Schrieffer[24] is $2.0kT_c$. Recent measurements[35–38] on tin indicate that the size of the energy gap is closely equal to the predicted value. Hence, these measurements were not complicated by the excitation of superconducting electrons.

[32] Kip, Langenberg, Rosenblum, and Wagoner, Phys. Rev. **108**, 494 (1957).
[33] A. B. Pippard, Physica **19**, 765 (1953).
[34] B. N. Aleksandrov and B. I. Verkin, Zhur. Eksptl. i Teoret. Fiz. **34**, 1655 (1958) [translation: Soviet Phys. JETP **7**, 1137 (1958)].
[35] Biondi, Forrester, and Garfunkel, Phys. Rev. **108**, 497 (1957).
[36] R. E. Glover and M. Tinkham, Phys. Rev. **104**, 844 (1956).
[37] R. E. Glover and M. Tinkham, Phys. Rev. **108**, 243 (1957).
[38] P. L. Richards and M. Tinkham, Phys. Rev. Letters **1**, 318 (1958).

The results of this experiment therefore indicate that the phenomenological two-fluid model of superconductivity, upon which Serber's calculations are based, provides a fair description of the high-frequency electrical features of superconductivity over the range of frequencies investigated. Calculations made from the BCS theory for the extreme anomalous limit give a curve for $A(\nu)$ of the right general shape, but low in absolute value by about a factor of two. Preliminary calculations for the partially anomalous case of tin indicate that there will be still better agreement between theory and experiment when this calculation is complete.

VI. ACKNOWLEDGMENTS

It is a pleasure to acknowledge the contributions of Professor C. H. Townes in many helpful discussions on the microwave problems encountered; of Professor R. Serber in making available his calculations of the surface resistance of superconductors; of Stanley Zemon in several helpful discussions; of M. Bernstein in providing all but one of the magnetrons used in this experiment; and of Bruce J. Biavati, Alan T. Hirshfeld, Herbert A. Leupold, Claire Metz, and Stanley A. Zemon in assisting in making the measurements. Communications from P. B. Miller made possible the comparison of these results and the BCS theory.

PHYSICAL REVIEW VOLUME 116, NUMBER 2 OCTOBER 15, 1959

Vibrational Spectrum of Vanadium

D. N. SINGH AND W. A. BOWERS
Physics Department, University of North Carolina, Chapel Hill, North Carolina
(Received June 1, 1959)

A theoretical lattice vibration spectrum is calculated for vanadium, in order to compare with the spectrum measured by the elastic incoherent scattering of neutrons. The calculated spectrum shows three peaks, the upper two of which occur at frequencies agreeing with the frequencies of the two peaks in the experimental curve. The third peak is not present in the measured spectrum. The maximum frequency of the calculated spectrum is lower by about 15% than the measured value.

RECENTLY Eisenhauer *et al.*[1] have used the inelastic incoherent neutron scattering technique to measure the lattice vibration spectrum of vanadium. In the absence of any theoretical spectrum calculated specifically for vanadium, they confined themselves to making qualitative comparisons with the characteristics of body-centered lattice vibration spectra as found by Montroll and Peaslee[2] in their general analysis and by Fine[3] in his work on tungsten.

We present here the results of some calculations for vanadium. Since the single-crystal elastic constants have not been measured, we have used the following method to obtain them: assuming that the measured elastic moduli for polycrystalline material are related to the single-crystal constants through Voigt's average,[4] and knowing from the work of Corak *et al.*[5] the low-temperature value of the Debye temperature, we have three equations which can be solved for the three cubic elastic constants. We find two sets of solutions. To choose between them, we note that they correspond to anisotropy factors[6] A which are, respectively, about 3.7 and 0.32; and since all cubic metals for which data exist have values of A greater than unity, we choose the first set in preference to the second. Further evidence for this choice lies in its yielding a maximum frequency of the spectrum (using the model described below) in better agreement with experiment than that given by the other. The values of the elastic constants found in this way are:

$$c_{11}=12.35\times10^{11}\ \text{dynes/cm}^2,$$
$$c_{12}=\ 8.77\times10^{11}\ \text{dynes/cm}^2,$$
$$c_{44}=\ 6.58\times10^{11}\ \text{dynes/cm}^2.$$

Since the Cauchy relation $c_{12}=c_{44}$ is not satisfied, a central force model is inadequate; we therefore use a model involving noncentral interactions. For the body-centered cubic lattice, the most general model consistent with symmetry requirements has two independent atomic force constants for the nearest neighbors, two for the next nearest, and three for third nearest neighbors.[7] We choose to neglect third and higher neighbors,

[1] Eisenhauer, Pelah, Hughes, and Palevsky, Phys. Rev. **109**, 1046 (1958); see also A. T. Stewart and B. N. Brockhouse, Revs. Modern Phys. **30**, 250 (1958).
[2] E. W. Montroll and D. C. Peaslee, J. Chem. Phys. **12**, 98 (1944).
[3] P. C. Fine, Phys. Rev. **56**, 355 (1939).
[4] R. F. S. Hearmon, *Advances in Physics*, edited by N. F. Mott (Taylor and Francis, Ltd., London, 1956), Vol. 5, p. 323. We are indebted to Dr. H. B. Huntington for sending us values of the elastic moduli of vanadium.
[5] Corak, Goodman, Satterthwaite, and Wexler, Phys. Rev. **102**, 656 (1956).
[6] C. Kittel, *Introduction to Solid-State Physics* (John Wiley and Sons, Inc., New York, 1956), p. 95.
[7] G. Leibfried, *Handbuch der Physik* (Springer-Verlag, Berlin, 1955), Vol. 7, Part I, p. 152.